MAGNETOQUANTUM OSCILLATIONS IN A LATERAL SUPERLATTICE

Dieter Weiss

Max-Planck-Institut für Festkörperforschung
Heisenbergstr. 1, D-7000 Stuttgart 80, FRG

The low temperature magnetoresistance of a high mobility two-dimensional electron gas is dominated by Shubnikov-de Haas oscillations, reflecting the discrete nature of the electron energy spectrum. When a weak one- or two-dimensional periodic potential is superimposed on the two-dimensional electron gas a novel type of oscillations occurs which reflects the commensurability of the relevant lengths in these systems – the cyclotron orbit diameter at the Fermi energy and the period a of the periodic potential. In addition the electron mean free path l_e also plays a role since the effect is observable only in mesoscopic systems where l_e is significantly longer than the period a of the potential. The essential aspects of these novel commensurability oscillations are discussed here in detail, starting from the discussion of same basic magnetotransport properties in an unmodulated two-dimensional electron gas (2-DEG).

INTRODUCTION: MAGNETOTRANSPORT IN A 2-DEG

At the interface of GaAs-AlGaAs heterojunctions the electrons are localized in the direction perpendicular to the layers (z-direction) and form a two-dimensional electron gas where the electrons can move freely in the x-y plane. The confinement in z-direction leads to the formation of subbands. We consider the situation where only the lowest subband (E_0) is occupied. In such a system the density of states is constant (see e.g. Aoki, 1987). In the presence of a magnetic field, however, the electron motion is completely quantized with energy eigenvalues (with respect to E_0) given by

$$E_n = (n + \frac{1}{2})\hbar\omega_c, \qquad n = 0, 1, ..., \tag{1}$$

with the Landau quantum number n and the cyclotron frequency $\omega_c = eB/m^*$ where B is the magnetic field, and m* is the effective mass in GaAs equal to 0.067 m_0. The density of states (DOS) is a series of δ-functions which are, however, collision broadened due to scattering processes characterized by a linewidth Γ. Within the selfconsistent Born approximation (SCBA) (Ando and Uemura, 1974; Gerhardts, 1975) assuming only short-range scatterers (with δ-function like scattering potentials) the DOS is a series of semi-ellipses with linewidth $\Gamma = \sqrt{\frac{2}{\pi}\hbar\omega_c\frac{\hbar}{\tau}}$ where τ is the transport scattering time (time between two scattering events) and is connected to the electron mobility $\mu = \frac{e}{m^*}\tau$. Each of these Landau levels (LL) is occupied by N_L electrons per unit area

Electronic Properties of Multilayers and Low-Dimensional Semiconductors Structures
Edited by J. M. Chamberlain *et al.*, Plenum Press, New York, 1990

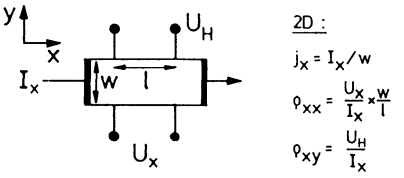

Figure 1. Determination of ρ_{xx} and ρ_{xy} by measuring the Hall voltage U_H and the voltage drop U_x along the applied current I_x in a Hall bar geometry. B is perpendicular to the plane.

given by $N_L = \frac{eB}{2\pi\hbar}$ (here spin splitting is included). The filling factor is defined as ratio between carrier density N_S and $N_L(\nu = N_s/N_L)$ and describes the occupancy of the Landau levels. For a homogeneous two-dimensional electron gas the wavefunction $|n, x_0\rangle$ of the electrons can be described as a plane wave in y-direction (Landau gauge $\vec{A} = (0, Bx)$) with wavenumber k_y ($\sim e^{ik_y y}$), and an eigenstate of a linear harmonic oscillator in the x-direction centered at $x_0 = -l^2 k_y$ (x_0 = center coordinate, l = magnetic length = $\sqrt{\hbar/eB}$). The extent of the wavefunction in x-direction is given by $2l\sqrt{2n+1}$ which for high quantum numbers n is the classical cyclotron diameter $2R_c = 2v_F/\omega_c = 2l^2 k_F$ where $k_F = \sqrt{2\pi N_S}$, the Fermi wavenumber.

A typical magnetoresistance experiment is sketched in Fig. 1. A constant current I_x is applied and the voltages U_x and U_H (Hallvoltage) are measured as a function of the magnetic field in z-directon. In a magnetic field the electric field $\vec{E}$ and the current density $\vec{j}$ are connected by the resistivity and conductivity tensor $\underline{\rho}$ and $\underline{\sigma}$, respectively:

$$\vec{E} = \underline{\rho}\vec{j} \text{ and } \vec{j} = \underline{\sigma}\vec{E}. \tag{2}$$

which are connected by

$$\underline{\rho} = \begin{pmatrix} \rho_{xx} & \rho_{xy} \\ \rho_{yx} & \rho_{yy} \end{pmatrix} = \frac{1}{\sigma_{xx}\sigma_{yy} - \sigma_{yx}\sigma_{xy}} \begin{pmatrix} \sigma_{yy} & -\sigma_{xy} \\ -\sigma_{yx} & \sigma_{xx} \end{pmatrix} \tag{3}$$

In a homogeneous 2DEG system the Onsager relation (Landau and Lifshitz, 1976) with $\sigma_{xx} = \sigma_{yy}$ and $\sigma_{yx} = -\sigma_{xy}$ holds. If $\sigma_{xx} = 0, \rho_{xx} = \sigma_{xx}/(\sigma_{xy}^2 + \sigma_{xx}^2)$ implies that $\rho_{xx} = 0$, simultaneously, which may sound strange but is true as long as $\sigma_{xy} \neq 0$ holds. Classically the conductivity components are given by the Drude formulas within the constant relaxation time approximation (τ = constant independent from DOS):

$$\sigma_{xx} = \frac{N_s e^2 \tau}{m^*} \frac{1}{1 + (\omega_c \tau)^2} \text{ and } \sigma_{xy} = -\frac{N_s e}{B} \frac{(\omega_c \tau)^2}{1 + (\omega_c \tau)^2}. \tag{4}$$

From this follows that the resistivity is independent of B, $\rho_{xx} = m^*/e^2 N_s \tau$. The magnetoresistance in a degenerate 2DEG, however, displays Shubnikov-de Haas (SdH) oscillations, reflecting the discrete nature of the degenerate Landau energy spectrum. Theoretically one has to go beyond the constant relaxation time approximation and consider a scattering rate τ which depends on the DOS. Within the SCBA one now

obtains an oscillating conductivity $\sigma_{xx} \propto e^2 D(E_F)^2$ (Ando and Uemura, 1974) which vanishes when the Fermi energy is between two LL's.

In the following it will be shown that a novel type of magnetoresistance oscillations arises when a 1-dimensional or 2-dimensional periodic potential is superimposed on a 2-DEG. The system under consideration is mesoscopic in the sense, that the period of the modulation potential is small compared to the mean free path of the electrons so that ballistic transport over several hills and valleys of the potential can take place.

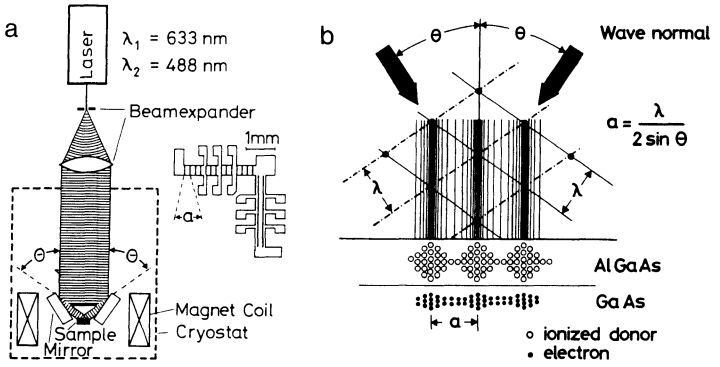

Figure 2. Schematic experimental set up (left hand side) and top view of the L shaped sample geometry where the interference pattern is sketched (a). Sketch of the spatial modulation of the concentration of ionized donors in the AlGaAs layer and of electrons in the 2-DEG produced by holographic illumination using two interfering laser beams with wavelength λ. The interference pattern created is shown schematically (b).

CREATION OF A LATERAL SUPERLATTICE: HOLOGRAPHIC ILLUMINATION

In selectively doped GaAs-AlGaAs heterostructures a persistent increase in the two-dimensional electron density is observed at temperatures below T = 150 K if the device is illuminated with infrared or visible light. This phenomenon is usually explained on the basis of the properties of DX-centers (persistent photoconductivity effect: PPC) which seem to be related to a deep Si donor. The increase in the electron density depends on the photon flux absorbed in the semiconductor so that a spatially modulated photon flux generates a modulation in the carrier density. In our measurements a holographic illumination of the heterostructure at liquid helium temperatures is used to produce a periodic potential with a period on the order of the wavelength of the interfering beams. In Fig.2b the interference of two plane light waves which create a periodic modulation of the ionized donors and therefore of the carrier density is shown schematically.

The existence of a periodically modulated carrier density in such structures has

been demonstrated by Tsubaki et al. (1984) who measured the anisotropy of the resistivity parallel and perpendicular to the interference fringes at 90 K. In the presence of a magnetic field, a new oscillatory phenomenon in such modulated systems is observed if one goes to lower temperatures, demonstrating clearly that a periodic modulation of the 2-DEG is present. The potential modulation obtained by this technique is on the order of 1meV where the Fermi energy E_F in our samples is typically 10 meV.

The samples used in the experiment were conventional GaAs-AlGaAs heterostructures grown by molecular beam epitaxy with carrier densities between $1.5 \cdot 10^{11} cm^{-2}$ and $4.3 \cdot 10^{11} cm^{-2}$ and low temperature mobilities ranging from $0.23 \cdot 10^6 cm^2/Vs$ to $1 \cdot 10^6 cm^2/Vs$. Illumination of the samples increases both the carrier density and the mobility at low temperatures. The heterojunctions discussed in the following sections consist of a semi-insulating GaAs substrate, followed by a 1μm-4μm thick undoped GaAs buffer layer, an undoped AlGaAs spacer (6nm-33nm), Si-doped AlGaAs (33nm-84nm), and an undoped GaAs toplayer ($\approx$ 22nm). We have chosen an L-shaped geometry (sketched on the right hand side of Fig.2a) to investigate the magnetotransport properties parallel and perpendicular to the interference fringes. Such a mesa structure was produced using standard photolithographic and etch techniques. Ohmic contacts to the 2-DEG were formed by alloying AuGe/Ni layers at 450°C. Some of the samples investigated have an evaporated semi-transparent NiCr front gate (thickness $\approx$ 8nm) or a back gate, respectively, in order to vary the carrier density after holographic illumination. Such a semi-transparent front gate is also essential for performing magnetocapacitance measurements after holographic illumination.

The experiment was carried out using either a 5mW HeNe laser (λ = 633 nm) or a 3 mW Argon-Ion Laser (λ = 488 nm) both linearly polarized. The experimental realization of the holographic illumination is shown schematically in Fig.2a. The laser system was mounted on top of the sample holder which was immersed in liquid helium (4.2 K) within a 10-Tesla magnet system. The laser beam which was expanded to a diameter of 40 mm entered the sample holder through a quartz window and a shutter. The shutter ensures well defined illumination times of the sample down to 25 ms. Short exposure times are important to prevent jumping of the fringes; therefore exposure times between 25 ms and 100 ms were typically chosen. The mirrors which split the laser beam into two coherent waves, are located close to the device and are arranged in such a way that an interference pattern with a period a is generated at the surface of the device. An aperture mounted above covers the sample from direct illumination. The period a of the fringes created in this way depends on the wavelength λ of the laser and the incident angle Θ (see Fig.2): $a = \lambda/2sin\Theta$. With the wavelengths used in this experiment we have realized periods between 282 and 382 nm for the interference pattern.

The advantage of this kind of "microstructure engineering" is its simplicity and the achieved high mobility of the microstructured sample due to the absence of defects introduced by the usual pattern transfer techniques (see e.g. Mauterndorf, 1988).

MAGNETORESISTANCE OSCILLATIONS: EXPERIMENTS

After holographic illumination of the sample which was carried out between 1.5 and 4.2 K, we have measured the resistivities and Hall resistances parallel and perpendicular to the grating using the L-shaped sample geometry (see Fig.2). We have chosen

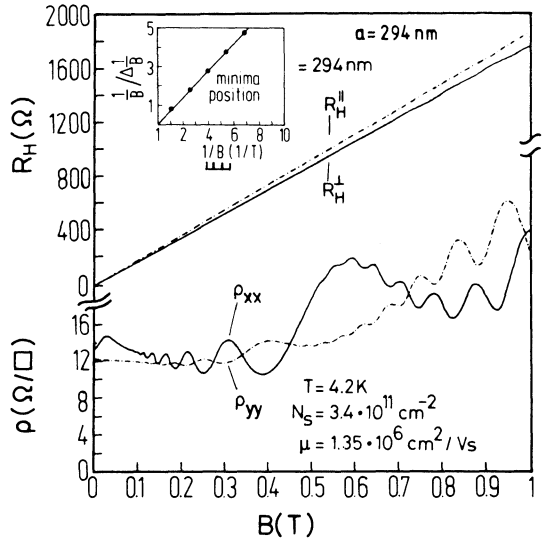

Figure 3. Magnetoresistivity ρ parallel (ρ_{yy}) and perpendicular (ρ_{xx}) to the interference fringes. The inset displays the 1/B dependence of the additional oscillations where the points correspond to minima in ρ_{xx}.

the x-axis to point in the direction perpendicular to the grating so that ρ_{xx} describes the transport perpendicular and ρ_{yy} parallel to the grating.

The magnetic field was perpendicular to the plane of the 2-DEG. The resistivities and Hall resistances are measured applying a constant current (1μA - 10μA) and measuring the voltage drop between potential probes along and perpendicular to the direction of current flow, respectively. A typical result obtained for a fringe period of $a = 294nm$ is shown in Fig.3. At magnetic fields above 0.5 T both ρ_{xx} and ρ_{yy} show the well known SdH-oscillations with a periodicity $\Delta(1/B)$ inversely proportional to the 2-DEG carrier density N_s. Below 0.5 T pronounced additional oscillations dominate ρ_{xx} while weaker oscillations with a phase shift of 180° relative to the ρ_{xx} data are visible in the ρ_{yy} measurements. The oscillations in ρ_{xx} are accompanied by a remarkable positive magnetoresistance at very low magnetic fields not present in ρ_{yy}. The Hall resistances, however, show no additional structure at magnetic fields below 0.5 T. Deviations from the clear linear behaviour of ρ_{xy} and ρ_{yx} occur only at magnetic fields above 0.5 T, and are connected to the SdH oscillations starting to be resolved. The slightly different slopes of ρ_{xy} and ρ_{yx} are due to a small difference in the carrier density of about 4% in the two branches of the sample.

A striking feature of this novel oscillations is their weak temperature dependence compared to SdH oscillations as is shown in Fig.4. At 13 K the additional oscillations in ρ_{xx} are still observable whereas the SdH oscillations are completely washed out. The strong temperature dependence of the SdH oscillations is due to the fact that their amplitudes depend on the Landau level separation $\hbar\omega_c$ as compared to the thermal energy k_BT. Therefore the additional oscillations do not originate from the Landau level separation $\hbar\omega_c$ as one would expect for electrons in higher subbands, e.g..

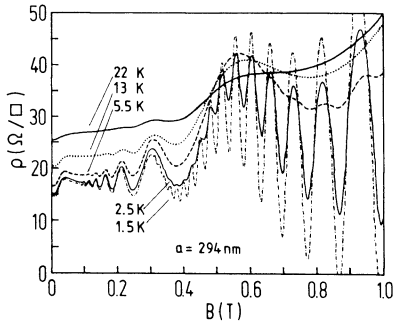

Figure 4. ρ_{xx} vs. B in the temperature range between 1.5 and 22K. The commensurability oscillations are less temperature dependent compared to the SdH-oscillations.

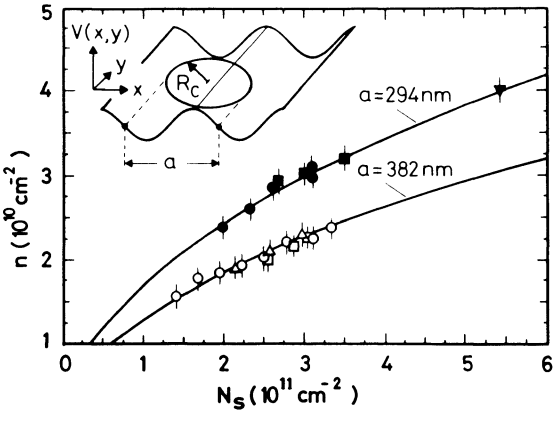

Figure 5. $n = \frac{e}{\pi\hbar}(\Delta\frac{1}{B})^{-1}$ versus N_s. Full symbols correspond to a laser wavelength λ=488nm, open symbols to λ=633nm and different symbols represent different samples. The solid lines are calculated using the condition that the cyclotron orbit diameter $2R_c$ is equal to an integer multiple of the interference period a, as is sketched in the inset.

The novel oscillations in ρ_{xx} and ρ_{yy} are perfectly periodic in 1/B as is demonstrated in the inset of Fig.3. The periodicity is obtained from the minima of ρ_{xx} which can be characterized by the commensurability condition

$$2R_c = (\lambda - \frac{1}{4})a, \qquad \lambda = 1, 2, 3, ..., \tag{5}$$

between the cyclotron diameter at the Fermi level, $2R_c$ and the period a of the modulation. For magnetic field values satisfying Eq.(5) minima are observed in ρ_{xx}. The periodicity $\Delta(1/B)$ can easily be deduced from Eq.(5) using the formulas given in the introduction:

$$\Delta\frac{1}{B} = e\frac{a}{2\hbar k_F} \tag{6}$$

where $\Delta(1/B)$ is the difference between adjacent minima (or maxima) of ρ_{xx} or ρ_{yy} on a 1/B scale.

The validity of Eq.(5) has been confirmed by performing these experiments on different samples, by changing the carrier density with an applied gate voltage, and by using two laser wavelengths in order to vary the period a. This is demonstrated in Fig.5 where the periodicity $\Delta(1/B)$ (displayed as carrier density $n = \frac{e}{\pi\hbar}(\Delta\frac{1}{B})^{-1}$) is plotted as a function of the carrier density N_s and the period a. The solid lines correspond to Eq.(6).

This simple picture is in excellent agreement with the experimental data displayed in Fig.5. To resolve an oscillation an elastic mean free path l_e at least as long as the perimeter of the cyclotron orbit is required. This agrees with our finding that the number of oscillation periods resolved depends on the mobility of the sample: the higher the mobility the more oscillations are observable since the electrons can traverse more periods of the potential ballistically. Similar experimental results have been observed recently by Winkler et al. (1989) using conventionally microstructured samples. The key for the explanation of this novel oscillatory behaviour of ρ_{xx} and ρ_{yy} in such periodically modulated 2-DEG's is a modification of the Landau level spectrum discussed in the next section.

LANDAU LEVELS IN A PERIODIC POTENTIAL: THEORY

The energy spectrum of electrons subjected to both a magnetic field and a periodic one-dimensional potential has been calculated by several authors (Aizin and Volkov, 1984; Kelly, 1985; Chaplik, 1985) using first order perturbation theory. Starting point is a Hamiltonian of the form

$$H = \frac{1}{2m^*}\left[-\hbar^2\frac{\partial^2}{\partial x^2} + \left(\frac{\hbar}{i}\frac{\partial}{\partial y} + \frac{e}{c}Bx\right)^2\right] + V_0 cos(Kx) \tag{7}$$

containing a periodic potential in x-direction $V(x) = V_0 cos(Kx)$ with period $a = 2\pi/K$. The energy spectrum can be taken in first order perturbation theory in V and is given

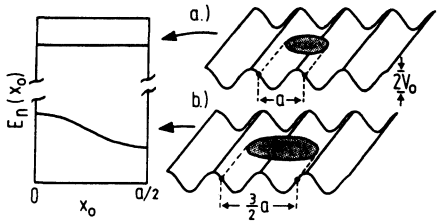

Figure 6. Simplified picture explaining the oscillating Landau level width.

by:

$$E_n(x_0) \approx (n + \frac{1}{2})\hbar\omega_c + \langle nx_0 \mid V(x) \mid nx_0 \rangle. \tag{8}$$

The right hand side matrix element can be regarded as effective potential acting on an electron averaged over the spatial extent of the wavefunction $\mid nx_0\rangle$ given by $2l\sqrt{2n+1}$ which is equal to the classical cyclotron diameter $2R_c$ for high quantum numbers n. Two extremal situations can be considered as is sketched in Fig.6. Assuming, for sake of simplicity, a stepfunction like wavefunction, the matrix element $\langle nx_0 \mid V(x) \mid nx_0\rangle$ at the Fermi energy vanishes when the cyclotron diameter equals an integer of the period a (Fig. 7a) leading to a flat Landau band, independent of the center coordinate x_0. On the other hand, a maximum contribution of the matrix element is expected for a cyclotron diameter equal to an odd integer of half the period a leading to Landau bands with strong curvature with respect to x_0 (Fig.6b). More precisely, the matrix element $\langle nx_0 \mid V(x) \mid nx_0\rangle$ can be calculated analytically giving

$$E_n(x_0) \approx (n + \frac{1}{2})\hbar\omega_c + U_n cos K x_0 \tag{9}$$

with $U_n = V_0 \exp(-\frac{1}{2}X)L_n(X)$ where $X = \frac{1}{2}K^2l^2$ and $L_n(X)$ stands for the n-th Laguerre polynominal. $L_n(X)$ is an oscillating function of both its index n and its argument X where the flat band situation (LL independent of x_0) is given by $L_n(X) = 0$. This flat band condition $L_n(X) = 0$ can be expressed in terms of the cyclotron radius R_c and is given by Eq.(5) (Gerhardts et al., 1989). A typical energy spectrum – calculated in first order perturbation theory – for $B = 0.8T, V_o = 1.5meV$ and $a = 100nm$ is plotted in Fig.7. The corresponding DOS is sketched on the right hand side in Fig.7. Note the double peak structure of the DOS at the band edges which one typically expects for a 1-D bandstructure due to the van Hove singularities. Near the Fermi energy E_F and for the parameter values of Fig.7 the first order approximation is excellent for $B > 0.1T$ but it breaks down for $B \to 0$ and has to be calculated numerically (Gerhardts, 1989).

The most important point here to understand is that a one-dimensional periodic potential lifts the degeneracy of the Landau levels and leads to Landau bands of finite

width. The bandwidth ($\approx 2U_n$) depends on the band index n in an oscillatory manner. The experimental verification of such a modified energy spectrum is the subject of the next section.

MODIFIED LANDAU LEVEL SPECTRUM: EXPERIMENTAL PROOF

In a two-dimensional electron gas the thermodynamic density of states $D_T(B)$ at the Fermi energy given by

$$D_T(B) = \frac{\partial N_s}{\partial \mu} = \int dE D(E) \frac{df(E-\mu)}{d\mu}, \tag{10}$$

where $f(x) = [\exp(x/kT) + 1]^{-1}$ is the Fermi function and the chemical potential μ is determined for a given electron density from $N_s = \int dE D(E) f(E-\mu)$. $D_T(B)$ is directly connected to magnetocapacitance $C(B)$ which is measured between gate and 2-DEG of the GaAs-AlGaAs heterojunction (Smith et al., 1985; Mosser et al., 1986):

$$\frac{1}{C(B)} = \frac{1}{C(0)} - \frac{1}{e^2 D_T(0)} + \frac{1}{e^2 D_T(B)}. \tag{11}$$

Here $D_T(0) = m^*/\pi\hbar^2$, the thermodynamic DOS at B = 0.

In a 2-DEG, $C(B)$ oscillates as a function of the magnetic field and the height of the magnetocapacitance maxima directly reflects the maximum value of the thermodynamic DOS at the Fermi energy which gives information about the Landau level width Γ. This has been used previously in homogeneous systems to investigate systematically the LL width Γ as a function of the electron mobility in such samples (Weiss and von Klitzing, 1987).

The active region of the sample used for the magnetocapacitance experiment was defined by etching a Hall-bar geometry and evaporating an 8 nm thick semi-transparent

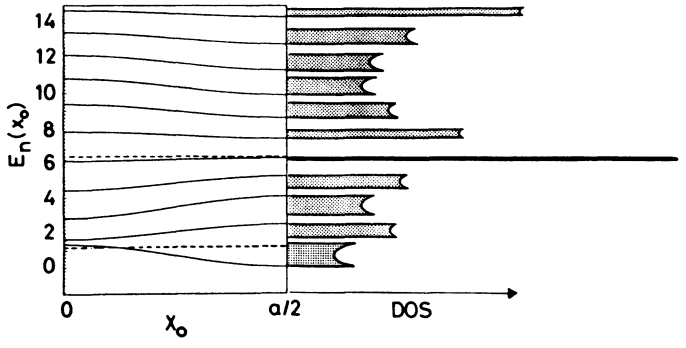

Figure 7. Calculated energy spectrum (first order perturbation theory) for B=0.8T, $V_0 = 1.5meV$ and a=100nm. The corresponding DOS is sketched. Flat parts of $E_n(x_0)$ lead to singularities in the DOS. The dashed lines correspond to the flat band situation determined by Eq.(5).

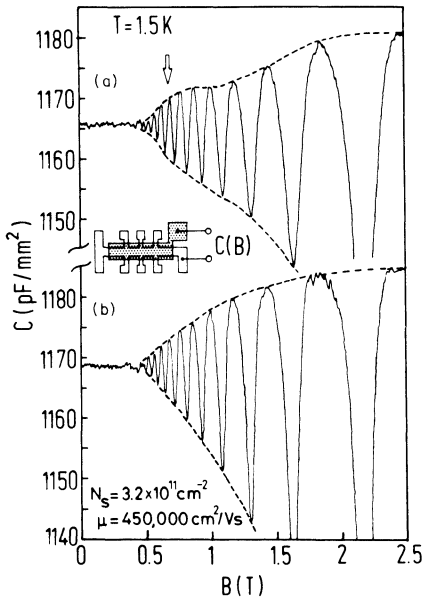

Figure 8. Measured magnetocapacitance (a) of a modulated sample compared to the capacitance of an essentially unmodulated sample (b). The arrow corresponds to the magnetic field value fulfilling Eq.5 for $\lambda = 1$. The inset sketches the measurement.

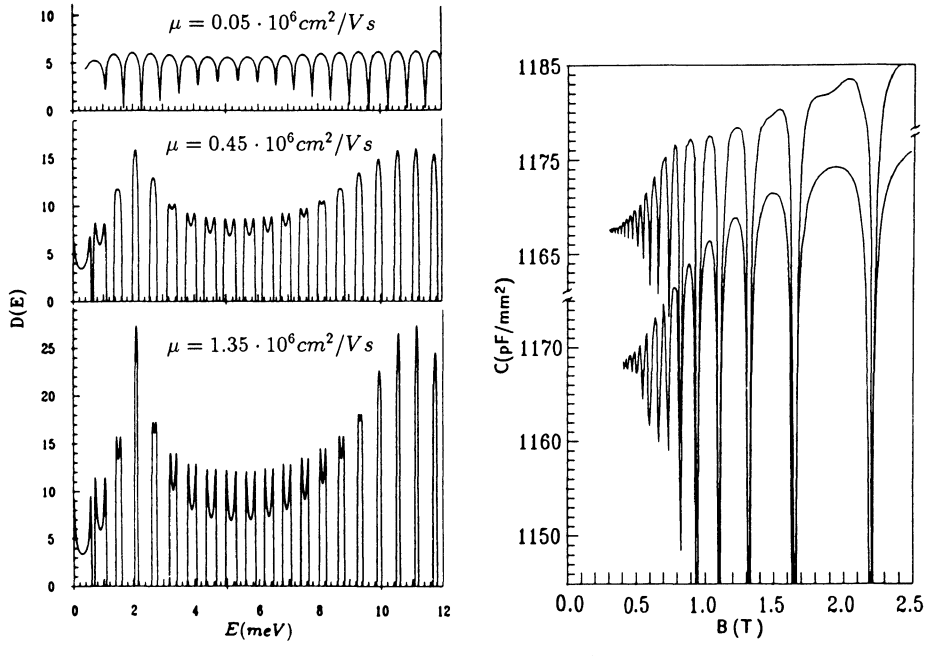

Figure 9. Calculated density of states in units of $m^*/\pi\hbar^2$ for several collision broadenings $\Gamma = \frac{e\hbar}{m^*}\sqrt{2B/\pi\mu}$ at B=0.35T and V_0=0.35meV.

Figure 10. Calculated magnetocapacitance versus magnetic field for $N_S = 3.2{\cdot}10^{11}cm^{-2}$ and $a = 365nm$. A B-independent linewidth is chosen to be $\Gamma = 0.3meV$. The upper curve is for $V_0 = 0.7meV$, and the lower one for the weak modulation $V_0 = 0.1meV$.

NiCr film as gate electrode. Prepared in such a way the sample shows a low temperature mobility of 240,000 cm^2/Vs and a carrier density of $1.5 \cdot 10^{11} cm^{-2}$ as has been determined by SdH oscillations and low field Hall measurements. After holographic illumination (duration 90 ms) using a 5mW HeNe laser which creates a periodic modulation with period $a = 365$ nm the carrier density was $3.2 \cdot 10^{11} cm^{-2}$ with a mobility of $450,000 cm^2/Vs$. The capacitance between the semi-transparent gate and the 2-DEG is measured with an ac-technique as sketched in Fig.8 (Smith et al., 1985; Mosser et. al., 1986). In a homogeneous 2-DEG it has been shown experimentally that the LL linewidth Γ has a magnetic field dependence of the form $\Gamma \propto B^{\alpha}$ with $0 \leq \alpha \leq 0.5$ (Weiss and von Klitzing, 1987; Gornik et al., 1985; Eisenstein et al., 1985), whereas theoretically $\Gamma \propto \sqrt{B}$ is expected for short range scatterers and Γ independent of B for long range scatterers (Ando and Uemura, 1974; Gerhardts, 1975). Since the Landau level degeneracy is proportional to B, the peak values of the DOS in the individual LL's and, as a consequence, the peak values of the capacitance are expected to increase monotonically with a structureless envelope with increasing magnetic field. On the other hand the envelope of the magnetocapacitance minima decreases monotonically with B due to the increasing LL separation $\hbar\omega_c$. In Fig.8 the magnetocapacitance data after an initial holographic illumination (a) is compared with the capacitance measured after an additional illumination which essentially smears out the periodic modulation (b). The carrier density in (b) has been adjusted to the same value as before the additional illumination using a negative gate voltage. In contrast to Fig.8b, where the magnetocapacitance behaves as usually observed in a 2-DEG, the capacitance oscillations in Fig.8a display a pronounced modulation of both the minima and maxima which is easily explained from the energy spectrum plotted in Fig.7. At about 0.69 T (marked by an arrow) the cyclotron diameter at the Fermi energy equals three quarter of the period a and corresponds to the last flat band situation ($\lambda = 1$). Therefore, the magnetocapacitance values near 0.69 T are approximately equal in Fig.8a and Fig.8b. If now the magnetic field is increased, broader Landau bands are swept through the Fermi level, and cause the nonmonotonic behaviour visible in Fig.8a. At higher magnetic fields the modulation broadening saturates and the usual LL degeneracy again raises the DOS in a LL with increasing field. It should be mentioned that in the magnetocapacitance the same modulation effect is observed for different angles between the one-dimensional modulation and the long axis of the Hall bar as is expected for a thermodynamic quantity in contrast, of course, to the magnetoresistivity. Note that below 0.69 T no oscillations comparable to those one observes in magnetotransport experiments are resolved. This behaviour will be considered in the next section.

The discussion of the magnetocapacitance up to now uses qualitative arguments rather than quantitative ones. In order to check the magnetocapacitance data theoretically, microscopic calculations of the DOS based on a generalisation of the well known selfconsistent Born approximation have been performed by Zhang (Weiss et al., 1989). In these calculations the energy spectrum of the homogeneous 2-DEG (e.g. Ando et al., 1982) – which leads to the semi-elliptic, n-independent shape of the density of states with a linewidth $\Gamma = \sqrt{\frac{2}{\pi}\hbar\omega_c\frac{\hbar}{\tau}}$ – is replaced by the energy spectrum obtained from Eq.(7) in first order perturbation theory where for each modulation broadened Landau band an average selfenergy is calculated. The resulting density of states is plotted in Fig.9 for different mobilities which characterize the collision induced linewidth broadening. In this approximation the double peak structure of the LL's due to the van Hove singularities is resolved if the collision broadening Γ is sufficiently small compared to the modulation broadening U_n. The oscillatory n-dependence of the modulation broadened LL's leads to an oscillation of the peak values of the DOS

with maxima for the narrowest levels. Once the DOS is calculated the data can be easily converted into magnetocapacitance data using Eq.(10) and Eq.(11). Calculating the magnetocapacitance for a modulation amplitude $V_0 = 0.7meV$ (Fig.10) reproduces the experimentally observed modulation of the envelope of the capacitance maxima (Fig.8a). A weaker amplitude of the periodic potential $V_0 = 0.1meV$ leads to the behaviour of the envelope usually observed in homogeneous 2-DEG's. The results of Fig.10 are obtained for a B-independent value $\Gamma = 0.3meV$, which yields a much better agreement with the experimental capacitance results than a linewidth calculated from the mobility μ according to the relation $\Gamma \propto (B/\mu)^{1/2}$ valid for short range scatterers. This phenomenon is well known for unmodulated samples of comparable mobility (Weiss and von Klitzing, 1987) and indicates the importance of long range scatterers (Ando and Uemura, 1974).

The van Hove singularities, not resolved experimentally in Fig.8a, are visible in the calculated data where a splitting of the Landau level is observed in the upper curve ($V_0 = 0.7meV$) at about 2 T.

The modified energy spectrum which has been proven experimentally in this section is the key for the explanation of the periodic potential induced oscillations given in the next section.

MAGNETORESISTANCE OSCILLATIONS: THEORY

The theory presented here follows closely the calculations of Gerhardts et al. (1989). The oscillations in ρ_{xx} (σ_{yy}) can be understood within a simple damping theory which means that electron scattering is described by a constant relaxation time τ. The k_y dispersion of the Landau energy spectrum leads to an additional contribution to the conductivity σ_{yy} which is within the framework of Kubo's formula (e.g. Kubo et al., 1965) given by

$$\Delta\sigma_{yy} = \frac{2e^2\hbar}{2\pi l^2}\int_0^a \frac{dx_0}{a}\sum_n \left(-\frac{1}{\gamma}\frac{df}{dE}(E_n(x_0)) \mid \langle nx_0 \mid v_y \mid nx_0\rangle \mid^2\right) \tag{12}$$

where $\gamma = \hbar/\tau$, f is the Fermi function, $\mid nx_0\rangle$ are the eigenstates of Eq.(7) and v_y is the velocity operator in y direction. These eigenstates carry current in the y direction

$$\langle nx_0 \mid v_y \mid nx_0\rangle = -\frac{1}{m^*\omega_c}\frac{dE_n}{dx_0} = \frac{1}{\hbar}\frac{dE_n}{dk_y} \tag{13}$$

but not in x-direction,

$$\langle nx_o \mid v_x \mid nx_o\rangle = 0, \tag{14}$$

which is the reason for the anisotropic behaviour of σ_{xx} (corresponding to ρ_{yy}) and σ_{yy} (corresponding to ρ_{xx}). In Eq.(13) the modified energy spectrum comes into play. The matrix element $\langle x_0n \mid v_y \mid x_0n\rangle$ vanishes always then when flat Landau bands (see e.g. Fig.7) are located at the Fermi energy, and $\Delta\sigma_{yy} = 0$. Consequently also $\Delta\rho_{xx}$ – the extra contribution to the resistivity ρ_{xx} – vanishes since $\Delta\rho_{xx} \approx \Delta\sigma_{yy}/\sigma_{xy}^2$ if $\omega_c\tau > 1$. On the other hand dE_n/dx_o displays a maximum value when the Fermi energy is located within the Landau band with the strongest dispersion and therefore $\Delta\sigma_{yy}$ ($\Delta\rho_{xx}$) is at maximum. A calculation based on the evaluation of Eq.12 which is compared to experimental magnetoresistivity data is shown in Fig. 11.

Assuming a modulation potential of 0.3 meV in the calculations reproduces nicely the oscillations of ρ_{xx} (solid lines in Fig.11). Note that the weak temperature de-

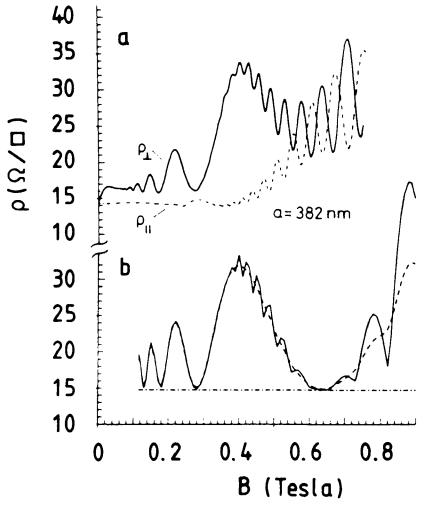

Figure 11. Magnetoresistivities for current perpendicular (ρ_{xx}, solid lines) and parallel (ρ_{yy}, dash-dotted lines) to the interference fringes, for a sample with $N_S = 3.16 \cdot 10^{11} cm^{-2}$, $\mu = 1.3 \cdot 10^6 cm^2/Vs$, and $a = 382nm$ – (a) measured at temperature $T = 2.2K$; (b) calculated for $T = 2.2K$ and for $4.2K$ (ρ_{xx} dashed line, ρ_{yy} shows no temperature dependence), using $V_0 = 0.3meV$ (Gerhardts et al., 1989).

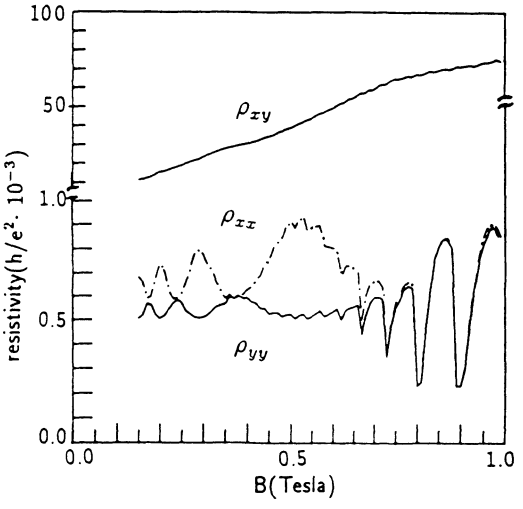

Figure 12. Calculated magnetoresistivity and Hall resistance for T=4.2K, a=294nm, $N_s = 3.14 \cdot 10^{11} cm^{-2}$, $\hbar/\tau$=0.0128meV and V_0=0.25meV. The oscillations in ρ_{yy} are due to a DOS dependent scattering rate so that $\rho_{yy} \propto e^2 D(E_F)^2$ (Gerhardts and Zhang, 1989).

pendence of the commensurability oscillations in ρ_{xx} (dashed line in Fig.11) is given correctly by the calculation in agreement with the experimental findings in Fig.4. The temperature dependence of these oscillations is much weaker than that of SdH oscillations, since the relevant energy is the distance between flat bands, which is much larger than the mean distance between adjacent bands. Winkler et al. (1989) have explained the oscillations in ρ_{xx} – measured in samples with microstructured gates – along very similar theoretical lines. Using the quasi-classical large-n limit, which means

$$e^{-\frac{1}{2}X} L_n(X) \approx \pi^{-\frac{1}{2}} (nX)^{-\frac{1}{4}} \cos\,(2\sqrt{nX} - \frac{\pi}{4}), \tag{15}$$

and assuming that $\hbar\omega_c < kT$ (high temperature limit) one can deduce their result from Eq.(12)

$$\Delta\sigma_{yy} \approx \frac{e^2}{2\pi\hbar} \frac{V_0^2}{\gamma\hbar\omega_c} \frac{4}{ak_F} \cos^2\,(2\pi\frac{R_c}{a} - \frac{\pi}{4}). \tag{16}$$

Eq.(16) can be rewritten to give $\Delta\rho_{xx}$ making use of the fact that $\Delta\rho_{xx} \approx \sigma_{yy}/\sigma_{xy}^2$:

$$\Delta\rho_{xx} \approx \frac{1}{2\pi\hbar} \frac{V_0^2}{\gamma\hbar\omega_c} \frac{4}{ak_F} \frac{B^2}{N_s^2} \cos^2\,(2\pi\frac{R_c}{a} - \frac{\pi}{4}). \tag{17}$$

Equation (17) may be used to estimate from the amplitudes $\Delta\rho_{xx}^{max}$ of the commensurability oscillations the amplitude of the superimposed periodic potential. From the maximum of ρ_{xx} at 0.41T (Fig.11a) one estimates $V_0 = 0.28meV$ in good agreement with the calculation in Fig.11b.

While the low field oscillations of ρ_{xx} are nicely reproduced by the calculation, the calculated ρ_{yy}-data (dashed-dotted line in Fig.11b) display simply the magnetic field independent Drude result in contrast to the experiment which shows maxima when the Landau bands are flat (DOS maximum at E_F). This is not too surprising since one cannot describe the usual SdH oscillations of a homogeneous 2-DEG within the

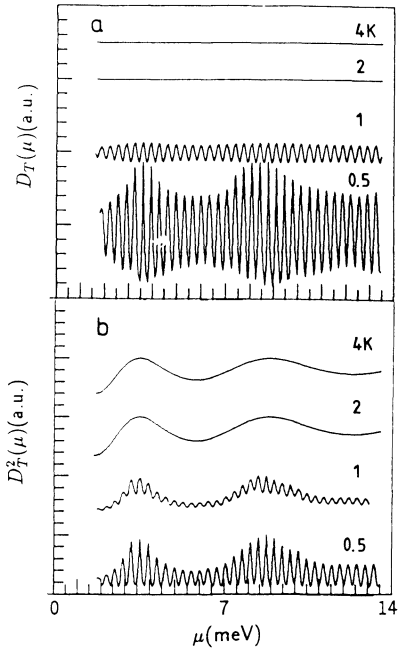

Figure 13. Thermal average of (a) DOS D(E), and (b) $D(E)^2$, versus chemical potential for different temperatures. The curves are normalized and shifted so that (a) the average value is 1, (b) the maximum value is 1. B=0.2T, V_0=0.25meV (Zhang and Gerhardts, 1989).

constant relaxation time approximation; you end up with the simple Drude result. The same result has been obtained by Beenakker (1989) using a semiclassical model (guiding center drift resonance). Beenakker noticed that the mean square Hall-drift velocity has an oscillating behaviour according Eq.(5) which, expressed as one-dimensional diffusion constant, leads via Einstein's law to the novel oscillations of ρ_{xx} while ρ_{yy} shows no magnetic field dependence. In order to understand the experimentally observed ρ_{yy} oscillations one has to go beyond this approximation - in analogy to the description of the SdH oscillations - and consider a density-of-state-dependent scattering rate. In the calculations one has to go through the formalism of the selfconsistent Born approximation (Ando and Uemura, 1974; Gerhardts, 1975) using the solutions of Eq.7. A detailed description of this theory has been given by Zhang and Gerhardts (1989). In analogy to the theory of SdH oscillations they find that

$$\sigma_{xx} \propto D_T^2(\mu) = \int dE \frac{df(E-\mu)}{d\mu} D(E)^2 \tag{18}$$

where $D_T^2(\mu)$ is the thermal average of the square of the DOS, not to be confused with the square of the thermodynamic DOS $D_T(\mu)$ defined in Eq.(10). Therefore, the weak antiphase oscillations in ρ_{yy} are in phase with the density of states oscillations and maxima in ρ_{yy} are always observed when the DOS at the Fermi-energy is at maximum, in contrast to ρ_{xx} which displays minima when the Landau bands are flat since $dE_n/dx_0 = 0$. Calculated curves of ρ_{xx} and ρ_{yy} are shown in Fig.12 demonstrating this behaviour in agreement with the experiment (Fig.3 and 11a). Eq.(18) also explains why the quantization of the Landau levels is essential for the explanation of the oscillations at least of ρ_{yy} while the quantization is not resolved in magnetocapacitance measurements at low magnetic fields. The reason for this is visualized in Fig.13 where

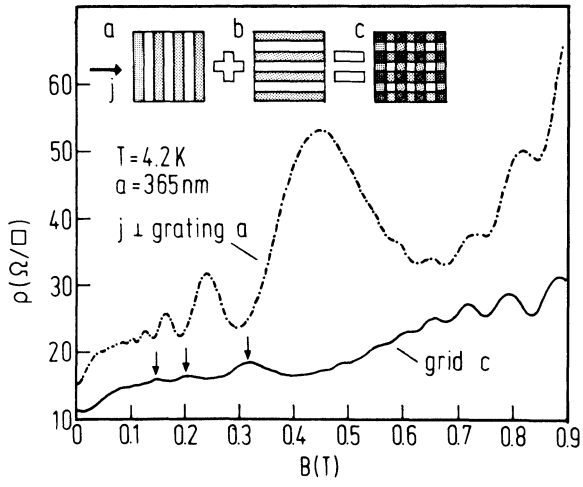

Figure 14. Magnetoresistance in a grating (j $\perp$ grating) and grid. The creation of the holographically defined pattern is shown schematically.

the thermodynamic density of states $D_T(\mu)$ (Eq.10) which determines the magnetocapacitance signal is compared to $D_T^2(\mu)$, the quantity which is responsible for the behaviour of ρ_{yy} (Eq.18). Up to 1K the Landau level quantization is resolved in $D_T(\mu)$ as well as in $D_T^2(\mu)$. At higher temperatures all the structure in D_T (which determines the magnetocapacitance) is washed out, $D_T^2(\mu)$, however, which determines ρ_{yy} shows still pronounced oscillations with maxima at flat band energies given by $2R_c = (\lambda - \frac{1}{4})a$.

MAGNETORESISTANCE IN A TWO-DIMENSIONAL PERIODIC POTENTIAL

In this last section some preliminary results of low field magnetotransport experiments in a two-dimensional periodic potential are presented. In such a potential grid the commensurability problem becomes more severe as compared to the 2-D case and results in a complicated energy spectrum (Hofstadter, 1976), and the shape of the DOS is not clear. The two-dimensional periodic potential ($V_0 \ll E_F$) with $a = 365nm$ is created by successively illuminating holographically a high mobility heterostructure ($\mu = 1.2 \cdot 10^6 cm^2/Vs$). Holographic illumination of type (a) in Fig.14 produces additional oscillations in the magnetoresistance as mentioned above (ρ_{xx}, dash-dotted line in Fig.14). An additional holographic illumination where the sample has been rotated by 90° results then in a grid potential sketched in Fig.14c. The magnetoresistance obtained under such conditions (solid line in Fig.14) displays a weak oscillating behaviour also corresponding to the commensurability condition Eq.(5), with maxima where ρ_{xx} –measured for situation (a)– shows minima. If one starts with an illumination of type (b) followed by (a) one ends up with the same result. The result obtained for the magnetoresistance in a two-dimensional periodic potential is therefore very close to the result one gets when the current flows parallel to the potential grating, discussed as additional oscillations in ρ_{yy} above (see e.g. Fig.3 and Fig.11). Therefore one may speculate that the DOS in a weak grid potential is similar to those in a grating and that the oscillating magnetoresistance (apart from SdH-oscillations) in a two-dimensional potential also reflects the oscillating scattering rate due to corresponding oscillations in the DOS according Eq.13.

ACKNOWLEDGEMENTS

I would like to thank K. v.Klitzing , R. R. Gerhardts, C. Zhang and D. Heitmann for valuable discussions and I am grateful to K. Ploog and G. Weimann for providing me with high quality samples.

REFERENCES

Aizin, G. R., and Volkov, V. A., Sov. Phys. JETP **60**, 844 (1984) [Zh. Eksp. Teor. Fiz **87**, 1469 (1984)]
Ando, T., and Uemura, Y., J. Phys. Soc. Jpn. **36**, 959 (1974)
Ando, T., Fowler, A. B., and Stern, F., Rev. Mod. Phys. **54**, 437 (1982)
Aoki, H., Rep. Prog. Phys. **50**, 655 (1987)
Beenakker, C. W. J., Phys. Rev. Lett. **62**, 2020 (1989)
Chaplik, A. V., Solid State Commun. **53**, 539 (1985)
Eisenstein, J. P., Störmer, H. L., Narayanamurti, V., Cho, A. Y., and Gossard, A. C., Phys. Rev. Lett. **55**, 1820 (1985), 539 (1985)
Gerhardts, R. R., Z. Physik **B21**, 285 (1975)
Gerhardts, R. R., Weiss, D., and von Klitzing, K., Phys. Rev. Lett. **62**, 1173 (1989)
Gerhardts, R. R., in "Science and Engineering of 1- and 0-Dimensional Semicondcutors", edited by S.P. Beaumont and C.M. Sotomayor Torres (Plenum, London), Proc. NATO ARW, 29 March - 1 April 1989, Cadiz, Spain, to be published
Gerhardts, R. R., and Zhang, C., Proc. Eighth Intern. Conf. Electronic Properties of Two-Dimensinal Systems, Grenoble, France, 4-8 Sept. 1989, to be published in Surf. Sci.
Gornik, E., Lassnig, R., Strasser, G., Störmer, H. L., Gossard, A. C., Wiegmann, W., Phys. Rev. Lett. **54**, 1820 (1985)
Gudmundsson, V., and Gerhardts, R. R., Phys. Rev. **B35**, 8005 (1987)
Hofstadter, D. R., Phys. Rev. **B14**, 2239 (1976)
Kelly, H. J., J. Phys. C. **18**, 6341 (1985)
Kubo, R., Miyake, S. J., and Hashitsume, N., Solid State Physics **17**, 239 (1965)
Landau, L. D., and Lifshitz, E. M., Course of Theoretical Physics vol. 5 (Oxford: Pergamon) 1976
Mauterndorf, 1988, Physics and Technology of Submicron Structures, Vol. 83 of Springer Series in Solid-State Sciences, ed. by H. Heinrich, G. Bauer, and F. Kuchar (Springer, Berlin, 1988)
Mosser, V., Weiss, D., von Klitzing, K., Ploog, K., and Weimann, G., Solid State Commun. **58**, 5 (1986)
Smith, T. P., Goldberg, B. B., Stiles, P. J., and Heilblum, M., Phys. Rev. **B32**, 2696 (1985)
Tsubaki, T., Sakaki, H., Yoshino, J., and Sekiguchi, Y., Appl. Phys. Lett. **45**, 663 (1984)
Weiss, D., and von Klitzing, K., in "High Magnetic Fields in Semiconductors Physics", Vol. 71 of Springer Series in Solid State Science, edited by G. Landwehr (Springer, Berlin, 1987), p. 57
Weiss, D., von Klitzing, K., Ploog, K., and Weimann, G., Europhys. Lett. **8**, 179 (1989); also in "The Application of High Magnetic Fields in Semiconductor Physics", ed. G. Landwehr, Springer Series in Solid State Sciences (Berlin), to be published
Weiss, D., Zhang, C., Gerhardts, R. R., von Klitzing, K., and Weimann, G., Phys. Rev. **B39**, 13030 (1989)
Weiss, D., von Klitzing, K., Ploog, K., and Weimann, G., Proc. Eighth Intern. Conf.

Electronic Properties of Two-Dimensional Systems, Grenoble, France 4-8 Sept. 1989, to be published in Surf. Sci.
Winkler, R. W., Kotthaus, J. P., and Ploog, K., Phys. Lett. **62**, 1177 (1989)
Zhang, C., and Gerhardts, R. R., submitted to Phys. Rev. B